Journal of Analytical and Applied Pyrolysis 96 (2012) 100–109

Contents lists available at SciVerse ScienceDirect

Journal of Analytical and Applied Pyrolysis

journal homepage: www.elsevier.com/locate/jaap

Influence of torrefaction on the devolatilization and oxidation kinetics of wood

M. Broström[a], A. Nordin[a], L. Pommer[a], C. Branca[b], C. Di Blasi[c,*]

[a] *Energy Technology and Thermal Process Chemistry, Umeå University, S-901 87 Umeå, Sweden*
[b] *Istituto di Ricerche sulla Combustione, C.N.R., P.le V. Tecchio, 80125 Napoli, Italy*
[c] *Dipartimento di Ingegneria Chimica, Università degli Studi di Napoli "Federico II", P.le V. Tecchio, 80125 Napoli, Italy*

ARTICLE INFO

Article history:
Received 17 January 2012
Accepted 20 March 2012
Available online 28 March 2012

Keywords:
Torrefaction
Wood
Kinetics
Decomposition
Oxidation

ABSTRACT

Devolatilization and oxidation kinetics of torrefied wood have been studied by evaluating thermogravimetric curves measured in nitrogen and air at various heating rates. Samples consist of Norway spruce wood chips torrefied at several process temperatures and residence times. Data about untreated wood have also been obtained for comparison. Measured curves are well predicted by means of a five-reaction mechanism, consisting of three devolatilization reactions for the pseudo-components hemicellulose, cellulose and lignin and, in air, of two additional reactions for char devolatilization and combustion. The torrefaction pre-treatment only requires model modifications in the amounts of volatiles generated from the decomposition of pseudo-components, indicating that only their relative percentages and not their reactivities are modified. On the other hand, a slightly different thermal stability is found for the char generated from torrefied wood, which results in higher activation energy and lower reaction order for the oxidation step. Hence torrefaction conditions can affect the subsequent conversion characteristics of the char product.

© 2012 Elsevier B.V. All rights reserved.

1. Introduction

The undoubted advantages of biomass fuels, associated with a reduced generation of SO_2 and NO_x and the neutrality in relation to CO_2 emissions, are accompanied by several drawbacks. These include high oxygen content resulting in a relatively low calorific value, low energy density, difficult handling and transportation, hygroscopic character with consequent high moisture levels, which again reduce the calorific value and give rise to degradation and self-heating during storage. The fibrous nature also gives rise to grinding and feeding difficulties.

Replacing fossil fuels with biomass is generally considered both efficient and cost-effective. Direct co-combustion is documented as promising and the most carbon efficient use of biomass materials [1]. Entrained flow gasification followed by synthesis of liquid products has further been identified as the most cost-efficient route from biomass to renewable liquid fuels [2–4]. Both combustion and gasification systems for coal are totally dominated by pulverized fuel systems, i.e. 98% of the coal-fired boilers are developed for coal powder [5] and 95% of the gasifiers in the world are dedicated for pulverized fuels [6]. Development of large-scale industrial refinement and distribution systems for biomass dedicated to powderized fuel systems are therefore needed to significantly contribute to combating the negative global trends. Industrial large-scale use of powderized biomass fuel has previously been severely hampered by several of the typical biomass inherent properties.

Among the pre-treatment technologies, to improve biomass properties, torrefaction has attracted noticeable interest in the last two decades [7], although it is not yet fully commercially proved on a large scale. It is a mild pyrolysis process, which takes place in a temperature range of about 473–593 K in an inert atmosphere and produces a material that, from the chemical point of view, presents a reduced O/C ratio. After torrefaction, higher energy density, increased grindability, improved feeding properties, improved hydrophobic character and generally higher product quality more resembling coal are attained. Also, biological activity is terminated, reducing risk of degradation, spontaneous combustion as well as spreading of invasive and non-indigenous species. The final powder fuel more resembles coal powder in terms of the factors mentioned, and may therefore be beneficial for the general end use process behavior.

A significant effort has been made to understand the effects of the torrefaction conditions on the product properties [7], but the important pyrolysis and combustion behavior of torrefied biomass has received little attention [8–11]. Different shapes and size distributions of powderized fuels as a result of the torrefaction pre-treatment may significantly change the reactivity. Furthermore, as torrefaction introduces changes in the structure of the material and reduces its volatile content, the yields of the pyrolysis products

---

[*] Corresponding author. Tel.: +39 081 7682232; fax: +39 081 2391800.
E-mail address: diblasi@unina.it (C. Di Blasi).

0165-2370/$ – see front matter © 2012 Elsevier B.V. All rights reserved.
http://dx.doi.org/10.1016/j.jaap.2012.03.011

are also modified at an extent that increases with the severity of the pre-treatment. Thermogravimetric measurements show that volatile release is displaced at higher temperatures and the shape of the corresponding curves is different mainly as a consequence of the action exerted by torrefaction on the hemicellulose component.

Kinetic analysis of thermogravimetric curves of biomass fuels, based on multi-step mechanisms [12,13], is needed for the design of thermochemical conversion systems. Moreover, kinetic models capable of describing measurements obtained at variable heating rates of samples representative of different thermal conditions can also be useful for optimizing the torrefaction process. Indeed, the changes induced by torrefaction on the main chemical components can appear as modified reaction mechanisms and kinetic constants. Unfortunately, kinetic models which take into account the devolatilization dynamics of hemicellulose, cellulose and lignin, already developed for biomass, have not yet been applied to torrefied material. Only one attempt has been made [8] to describe the thermogravimetric curves in air of torrefied wood. However, the mechanism simply consists of two global reactions (devolatilization followed by combustion) and is purely empirical because the parameter estimation is not carried out for the various experiments simultaneously. Instead the estimated parameters are specific for each single experiment. Moreover the thermogravimetric curves are obtained for one heating rate only, so that compensation effects are not avoided [14].

In this study spruce wood chips torrefied at different process temperatures and residence times are subjected to thermogravimetric analysis in both inert and oxidative environments at different heating rates. A simultaneous kinetic analysis of the resulting curves is carried out to formulate multi-step reaction mechanisms and to estimate the related kinetic parameters.

2. Materials and methods

2.1. Materials

Stem wood of Norway spruce, a coniferous tree, consisting of 42% cellulose, 26% hemicellulose, 31% lignin and 1% extractives (determined according to standards SCAN-CM 71:09, Tappi T222 and SCAN-CM 49) is used as feedstock. The wood chips are torrefied in a pilot plant in inert atmosphere. Dry wood chips with a maximum thickness of 4.5 mm are fed into an electrically heated rotating drum in which the torrefaction temperature and residence time are controlled. The filling is kept at a constant level, and therefore the mass flow of wood chips varies (4–12.5 kg/h) for the different residence times. This results in slightly different gas temperature profiles for the different residence times. In order to reach well defined conditions, the biomass is pre-heated prior to the torrefaction drum (final temperatures around 423–473 K for residence times of approximately 2–4 min). This is done in order to decrease the time for heating the biomass to the final torrefaction temperature, i.e. interfering with the measured residence time as little as possible. Since the pre-heating temperature is below where significant weight loss starts (473 K), it is considered to be sufficiently low not to interfere with the results. Gas temperatures are measured and controlled at five points in the torrefaction drum resulting in a well defined gas temperature profile. The torrefaction process temperature, T_p, used in the current study is the surface temperature on the torrefied wood chips at the end of the drum measured using an IR-pyrometer. The actual temperature inside the wood chips is not measured for practical reasons.

After the torrefaction zone, the torrefied wood chips are cooled. The torrefaction process conditions used for this study are designed to cover residence times (t_r) between 8 and 25 min and process temperatures (T_p) between 533 and 583 K, to produce materials spanning from lightly to severely torrefied. Residence time is the transport time of the biomass through the heated torrefaction drum, including also heating of the wood chips to the final torrefaction temperature. These figures lead to maximum heating rates (referred to the particle surface), limited to the torrefaction process, around 5–20 K/min. In reality, actual heating rates may be significantly higher owing to non-linear temperature rise with time and the possible existence of an isothermal period.

The chief sample characteristics (ash content, proximate analysis, elemental analysis, energy and mass yields, higher and lower heating values (HHV, LHV)) are summarized in Table 1, which also includes the information about the untreated wood used for comparison. Five torrefied samples are considered (a)–(e), which are ordered with increasing thermal severity of the torrefaction process (process temperature and residence time) as resulting, a posteriori, from the determined fixed carbon and C contents.

Proximate analysis indicates that the volatile content of the sample is decreased by the torrefaction process (from about 85 to 51%) to the advantage of fixed carbon and ash content. Both the temperature and residence time have a beneficial effect in this regard. As expected, the C content is also increased (from about 50 to 69%) with a consequent decrease in the H and O contents whereas the N content remains constant.

The calorific heating values HHV and LHV are measured and calculated according to the standardized procedure EN 14918. Heating values increase with the severity of the torrefaction, primarily as a result of the lowered oxygen content in the fuel. The dry, ash free (daf) solid mass (η_m) and energy yields (η_E) of the samples are defined as in previous torrefaction studies [9,10]:

$$\eta_m = \left(\frac{m_{\text{tor}}}{m_{\text{feed}}}\right)_{\text{daf}} \tag{1}$$

$$\eta_E = \eta_m \left(\frac{\text{HHV}_{\text{tor}}}{\text{HHV}_{\text{feed}}}\right)_{\text{daf}} \tag{2}$$

where m_{tor}, m_{feed}, HHV_{tor} and HHV_{feed} are the mass and the HHV of torrefied and fed wood, respectively. The mass yields decrease with increased thermal severity as a direct consequence of the partial devolatilization during the process (from 97 to 46% for the range of experimental conditions). Energy yield measures the solid energy efficiency of the process. It is the combination of increased heating value and decreased mass of the wood. Even though the mass loss is somewhat compensated for by increasing HHV of the product, the total energy yield decreases with the severity of the torrefaction conditions (from about 99 to 63%).

2.2. Apparatus and procedure

A TA Instruments Q5000IR apparatus is employed for the thermogravimetric measurements. This apparatus detects the mass loss with a sensitivity <0.1 μg. The temperature is measured at a position below the sample holder and is calibrated with a Curie point method involving 5 standardized alloys covering the temperature range of the measurements. Repeated calibrations are performed for the different heating rates. The wood samples are milled and ground to particle size <30 μm and a 3 mg sample is evenly spread in a 100 ml ceramic (Al_2O_3) sample pan. The sample is purged with a flow rate of totally 50 ml/min (10 ml/min from the balance housing and 40 ml/min from the sample purge inlet). Pure nitrogen is used for the devolatilization tests. For the evaluations under oxidizing conditions, the sample purge gas consists of a mixture of nitrogen and oxygen that results in total oxygen concentration (including the balance purge) of 21%, henceforth called air.

The experiments start with purging (room temperature for 30 min) followed by a drying session (rapid heating up to 378 K with a holding time of 15 min). A first set of experiments is carried out

Table 1
Properties of untreated wood and wood torrefied at several process temperatures, T_p, and residence times, t_r (samples (a)–(e)).

T_p [K], t_r [min]	Untreated wood	(a) 533, 8	(b) 533, 25	(c) 558, 16.5	(d) 583, 8	(e) 583, 25
Ash content %	0.23	0.3	0.4	0.4	0.4	0.7
Fixed carbon %	14.6	15.7	19.3	22.3	23.4	47.8
Volatiles %	85.4	84	80.3	77.3	76.2	51.5
C %	50.3	51.4	53.6	55.2	55.8	69.2
H %	6.2	5.9	5.9	5.6	5.8	5
O %	43.2	42.3	40	38.7	37.9	25
S %	<0.01	<0.01	<0.01	<0.01	<0.01	0.01
Cl %	<0.01	<0.01	<0.01	<0.01	<0.01	<0.01
N %	0.1	0.1	<0.1	0.1	0.1	0.1
Energy yield %	100	98.8	94.5	87.9	84.5	62.8
Mass yield %	100	97.1	89.2	80.3	76.5	45.9
HHV [MJ/kg]	20.3	20.6	21.5	22.2	22.4	27.8
LHV [MJ/kg]	19.0	19.4	20.2	21.0	21.1	26.7

in nitrogen. Thermogravimetric curves are determined for all the samples, including untreated wood, for a heating rate of 5 K/min and a final temperature 873 K. Furthermore, for untreated wood and one torrefied sample, representative of the typical torrefaction conditions (sample (b) with $T_p = 533$ K and $t_r = 25$ min, indicated in the following as "reference torrefied" wood), measurements are also made for heating rates of 2.5 and 10 K/min. A second similar set of experiments is repeated in air.

2.3. Kinetic modeling

Lignocellulosic fuel devolatilization and combustion have been extensively modeled assuming that volatiles are released according to a set of parallel reactions for lumped components [12,13,15]. Then, the overall mass loss rate is a linear combination of the single component rates. In air, weight loss curves show two main reaction zones attributed to decomposition of wood and heterogeneous oxidation of the char produced. The stage of char oxidation is, of course, absent for the curves obtained in inert atmosphere. A general kinetic mechanism is proposed here which includes decomposition, described by three reactions for the pseudo-components hemicellulose, cellulose and lignin [12–14,16–24] (only these steps are being used for the analysis of the curves obtained under a nitrogen flow) and oxidation, described by two reactions for char devolatilization and oxidation [25–30]:

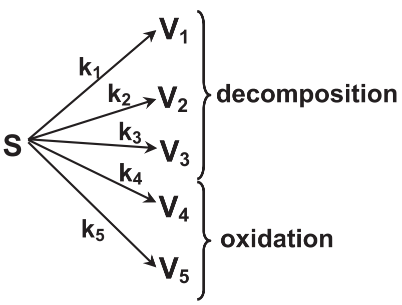

(a1)

(a2)

(a3)

(a4)

(a5)

where S is the sample which produces the lumped volatile products V_i ($i = 1, \ldots, 5$). The term "pseudo-component" is used as it is impossible in kinetic analysis to avoid overlap between different components in the measured weight loss curves [13], although in torrefaction the contribution of hemicellulose is expected to become lower. From the physical point of view, sample decomposition and char oxidation are sequential processes. The parallel reaction mechanism (a1)–(a5) is general as it can easily guarantee this feature by an appropriate set of parameter values and, at the same time, can describe well the possible overlap between the various reactions. Moreover, the estimated kinetic constants with the two approaches are approximately the same [31,32].

The reactions rates present the usual Arrhenius dependence (A_i are the pre-exponential factors and E_i the activation energies) on the temperature and a linear (decomposition and char devolatilization, n_1–$n_4 = 1$) or a power law with exponent n_5 (char oxidation) dependence on the mass fractions of lumped volatile species released. The latter treatment takes into account the evolution of the pore surface area during conversion [15]. Since the sample temperature, T, is a known function of time ($T = T_0 + h\,t$, T_0 is the initial temperature, h is the heating rate and t is time), the mathematical model consists of 5 ordinary differential equations for the mass fractions, Y_i, of the reacting solid fuel:

$$\frac{\partial Y_i}{\partial t} = -A_i \exp\left(\frac{-E_i}{RT}\right) Y_i^{ni}, \quad Y_i(0) = \nu_i, \quad i = 1, \ldots, 5 \qquad (3\text{–}7)$$

where ν_i, indicated in the following as stoichiometric coefficients, are the initial mass fractions of the lumped classes of volatiles generated.

The kinetic parameters are estimated through the numerical solution of the mass conservation equations and the application of a direct method for the minimization of the objective function, which considers both integral (TG) and differential (DTG) data, following the method already described [33]. The simultaneous use of experimental data measured for several heating rates avoids possible compensation effects in the kinetic parameters. The parameters to be estimated for the decomposition and oxidation steps are the activation energies (E_1–E_5), the pre-exponential factors (A_1–A_5), the stoichiometric coefficients (ν_1–ν_5) and the reaction order (n_5). Deviations between measurements and model predictions, dev_{TG} and dev_{DTG}, are defined as in [33].

3. Results and discussion

Some characteristic parameters (characteristic reaction temperatures, devolatilization rates and mass fractions) are introduced first to describe the thermogravimetric curves for all samples and reaction conditions considered. Then results are presented of the kinetic analysis with a comparison between measurements and predictions.

3.1. Devolatilization characteristics

The mass fraction, Y, and the time derivative of the mass fraction, $-dY/dt$ (indicated as TG and DTG curves in the following) are reported as functions of temperature in Fig. 1A and B for the various samples, as obtained under a nitrogen flow and a heating rate of 5 K/min. As expected, the DTG curve of untreated wood shows a "shoulder" associated with hemicellulose decomposition, followed by the attainment of a maximum, mainly due to cellulose decomposition, a rapid decay and a long tail. The wide range of temperatures, where lignin decomposes, hinders the appearance

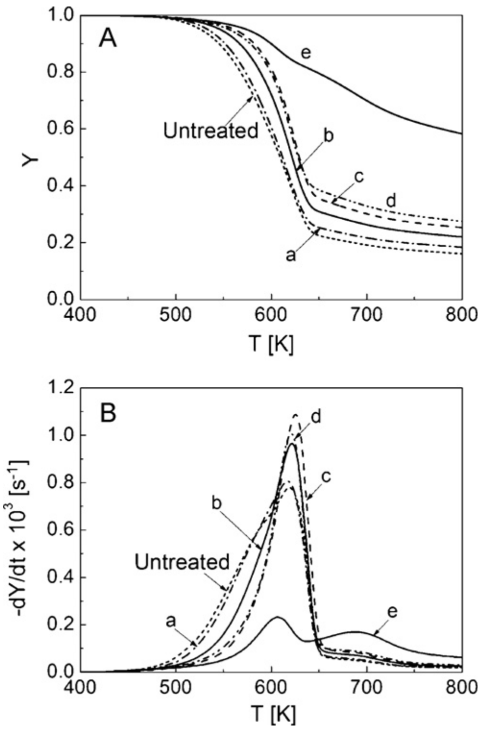

Fig. 1. Mass fraction (A) and time derivative of the mass fraction (B) as functions of temperature as measured for untreated wood and wood torrefied at various process temperatures, T_p, and residence times, t_r (nitrogen, heating rate 5 K/min up to 873 K): (a) $T_p = 533$ K, $t_r = 8$ min, (b) $T_p = 533$ K, $t_r = 25$ min, (c) $T_p = 558$ K, $t_r = 16.5$ min, (d) $T_p = 583$ K, $t_r = 8$ min, (e) $T_p = 583$ K, $t_r = 25$ min.

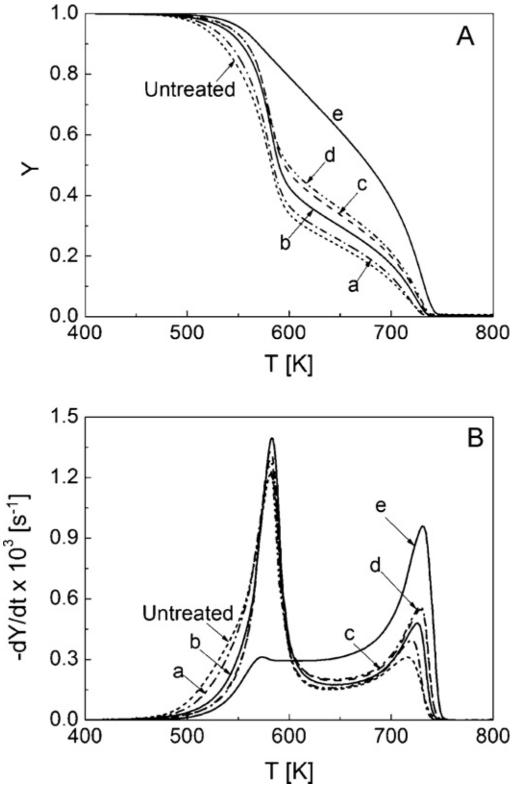

Fig. 2. Mass fraction (A) and time derivative of the mass fraction (B) as functions of temperature as measured for untreated wood and wood torrefied at various process temperatures, T_p, and residence times, t_r (air, heating rate 5 K/min up to 873 K): (a) $T_p = 533$ K, $t_r = 8$ min, (b) $T_p = 533$ K, $t_r = 25$ min, (c) $T_p = 558$ K, $t_r = 16.5$ min, (d) $T_p = 583$ K, $t_r = 8$ min, (e) $T_p = 583$ K, $t_r = 25$ min.

of a peak attributable to this component. Also, volatile evolution at very low temperatures is usually associated with decomposition of extractives. Differences between curves for untreated wood and wood obtained for very mild torrefaction conditions (sample (a) with $T_p = 533$ K and $t_r = 8$ min) are small. Then, as the torrefaction conditions become more severe, the shoulder in the DTG curve tends to disappear and the yields of solid residue become higher.

The TG and DTG curves obtained for untreated and torrefied wood in air at a heating rate of 5 K/min are reported versus temperature in Fig. 2A and B. In all cases, the process consists of a first devolatilization stage and a second stage of char oxidation, both associated with peaks in the rate of weight loss curves. As for the first stage, compared with the measurements carried out in nitrogen, the peak appears to be anticipated at lower temperatures and is much higher, confirming the ability of oxygen to enhance degradation of cellulose especially at low temperatures [34]. Also, it can be understood that the decomposition of the three main chemical components becomes more overlapped. Indeed the curves in air, even for untreated wood, do not show a clearly visible shoulder attributable to hemicellulose dynamics. The oxidation zone is characterized, at intermediate temperatures, by a wide region of low, almost constant rate, and at higher temperatures by the attainment of a second peak. This increases with the yields of char generated from both the torrefaction process and the oxidative decomposition during thermal analysis.

The degradation characteristics of the different samples can be quantified through several parameters, introduced in [21,26] and listed in Table 2A (all the curves at a heating rate of 5 K/min in nitrogen) and Table 2B (all the curves at a heating rate of 5 K/min in air), which are related to the temperature ranges of the different zones of the weight loss curves, (with the corresponding mass fractions and devolatilization rates), and the char yield. These include, for the curves obtained in nitrogen, the initial degradation temperature, T_{initial}, corresponding to a mass fraction of 0.975, the temperature T_{peak1}, where the maximum devolatilization rate is attained (associated mainly with cellulose decomposition), with the corresponding $-(dY/dt)_{\text{peak1}}$ and Y_{peak1}, and the beginning of the final, tailing region identified by $T_{\text{offset(c)}}$ (extrapolation of the devolatilization rate, corresponding to the local minimum in $-d^2Y/dt^2$ in this region, to the zero level of the Y axis). In addition to these parameters, for the curves obtained in air, the temperature T_{peak2}, where the second peak in the rate of weight loss is attained, and the corresponding $-(dY/dt)_{\text{peak2}}$ and Y_{peak2} are introduced. The char yields, Y_c, are also defined for the two cases as the solid mass fraction detected for $T = 773$ K (nitrogen), or the mass fraction in correspondence of the rapid decay of the rate after the first peak (air). The parameters associated with hemicellulose decomposition are not introduced as they cannot be exactly defined except for the curves of untreated wood and sample (a) in nitrogen, owing to the modifications introduced in this component by torrefaction and/or the overlap of its shoulder with the cellulose peak.

For both reaction environments, the T_{initial} values are displaced to successively larger values starting from untreated wood to torrefied wood at successively higher process temperatures and/or residence times, most likely owing to the changes in the more labile components, extractives, hemicellulose and lignin. As already observed, oxidative degradation is anticipated (502–539 K) with respect to thermal degradation (509–544 K). The first peak temperature is not significantly altered by the torrefaction process, although the values are lower in air (573–583 K versus 607–625 K). The maximum peak rate first becomes slightly higher (absolute maximum for sample (c)) and then decreases, indicating a change in the chemical composition/structure of samples (values are significantly higher in air). The beginning of the tailing zone ($T_{\text{offset(c)}}$) is

Table 2A
Characteristic parameters of the thermogravimetric curves measured in nitrogen at a heating rate of 5 K/min for untreated wood and wood torrefied at several process temperatures, T_p, and residence times, t_r (see the notation in the text).

Parameters	Torrefaction conditions (T_p [K], t_r [min])					
	Untreated wood	(a) 533, 8	(b) 533, 25	(c) 558, 16.5	(d) 583, 8	(e) 583, 25
T_{initial} [K]	509	516	525	538	532	544
T_{peak1} [K]	619	618	622	625	621	607
Y_{peak1}	0.41	0.44	0.50	0.55	0.85	0.88
$-(dY/dt)_{\mathrm{peak1}} \times 10^3$ [s^{-1}]	0.78	0.81	0.97	1.09	1.01	0.23
$T_{\mathrm{offset(c)}}$ [K]	649	647	648	651	647	–
Y_c	0.17	0.19	0.23	0.26	0.29	0.60

Table 2B
Characteristic parameters of the thermogravimetric curves measured in air at a heating rate of 5 K/min for untreated wood and wood torrefied at several process temperatures, T_p, and residence times, t_r (see the notation in the text).

Parameters	Torrefaction conditions (T_p [K], t_r [min])					
	Untreated wood	(a) 533, 8	(b) 533, 25	(c) 558, 16.5	(d) 583, 8	(e) 583, 25
T_{initial} [K]	502	509	519	528	526	539
T_{peak1} [K]	582	581	583	582	580	573
$-(dY/dt)_{\mathrm{peak1}} \times 10^3$ [s^{-1}]	1.22	1.29	1.39	1.33	1.26	0.31
Y_{peak1}	0.51	0.55	0.61	0.65	0.68	0.89
T_{peak2} [K]	716	720	726	728	728	731
$-(dY/dt)_{\mathrm{peak2}} \times 10^3$ [s^{-1}]	0.31	0.40	0.48	0.55	0.56	0.96
Y_{peak2}	0.06	0.05	0.05	0.06	0.07	0.12
$T_{\mathrm{offset(c)}}$ [K]	599	598	598	598	596	584
Y_c	0.34	0.37	0.44	0.49	0.52	0.85

also not affected by the torrefaction process, but it is again displaced at lower values for the measurements in air (596–599 K versus 647–651 K). The more severe the conditions of the torrefaction pretreatment are the higher is the solid mass fraction evaluated at the characteristic points of the thermogravimetric curves, including the char yield. This is due to the presence of successively larger amounts of char in the sample that is then subjected to further degradation under thermogravimetric conditions. Consequently, the peak of the oxidation rate also becomes higher with a small increase in the corresponding temperature (from 716 to 731 K).

The influence of the heating rate (2.5–10 K/min) on the measured curves is summarized through the characteristic parameters listed in Table 3A and Table 3B for the untreated and the reference torrefied wood in nitrogen and air. The differences due to the reaction environment and the torrefaction conditions remain qualitatively the same but, as already well known for untreated wood [13], T_{initial} and the peak temperatures are displaced toward higher values (for instance, T_{peak1} in the range 609–634 K (nitrogen) or 570–595 K (air) for the range of heating rates considered). Moreover, the peak rates also become progressively higher while the char yields generally tend to diminish with increased heating rate.

3.2. Kinetic analysis of the curves obtained in inert environment

The kinetic evaluation for the thermal devolatilization (nitrogen) is carried out, in the first place, for the untreated wood, using the measurements obtained at heating rates of 2.5, 5 and 10 K/min and using as starting values of the parameters those already determined in [21] for the same wood species at a single heating rate of 5 K/min. It is found that the three-step mechanism produces good predictions of the devolatilization process with parameters (Table 4) that are very close to those previously estimated (activation energies for the three pseudo-components of 101, 213 and 39 kJ/mol versus 100, 236 and 46 kJ/mol). These small differences can be attributed to the different geographical origin, age and specific part of the tree [22]. As reported in previous studies [13], the amount of volatiles generated from the decomposition of the three pseudo-components slightly increases with the heating rate. However, given the small differences, average values (Table 4) can be used. An example of the predicted process dynamics for untreated wood, in terms of the three pseudo-components, and a comparison between prediction and measurements is shown in Fig. 3A and B.

The set of kinetic parameters obtained for the thermal devolatilization of untreated wood is used to start the evaluation of the thermogravimetric data for the reference torrefied wood

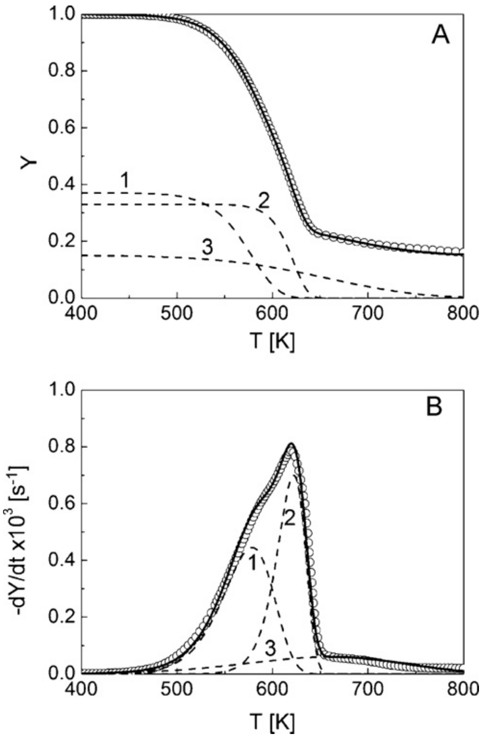

Fig. 3. Comparison between the observed (symbols) and simulated TG (A) and DTG (B) curves (solid lines) for untreated wood. Thin lines with various styles denote the predicted evolution of the mass fraction and the time derivatives of the pseudo-components (nitrogen, heating rate 5 K/min up to 873 K; 1,2,3: decomposition of pseudo-components hemicellulose, cellulose and lignin).

Table 3A
Characteristic parameters of the thermogravimetric curves measured in nitrogen at three heating rates, *h*, for untreated wood and the reference torrefied wood (sample (b)).

Parameters	Untreated wood *h* [K/min]			Reference torrefied wood (sample (b)) *h* [K/min]		
	2.5	5	10	2.5	5	10
T_{initial} [K]	500	509	513	517	525	532
T_{peak1} [K]	609	619	633	611	622	634
Y_{peak1}	0.40	0.41	0.39	0.50	0.50	0.50
$-(dY/dt)_{\text{peak1}} \times 10^3$ [s^{-1}]	0.40	0.78	1.48	0.50	0.97	1.82
$T_{\text{offset(c)}}$ [K]	635	649	661	632	648	659
Y_c	0.18	0.17	0.17	0.23	0.23	0.24

Table 3B
Characteristic parameters of the thermogravimetric curves measured in air at three heating rates, *h*, for untreated wood and the reference torrefied wood (sample (b)).

Parameters	Untreated wood *h* [K/min]			Reference torrefied wood (sample (b)) *h* [K/min]		
	2.5	5	10	2.5	5	10
T_{initial} [K]	494	502	507	520	519	526
T_{peak1} [K]	570	582	594	570	583	595
$-(dY/dt)_{\text{peak1}} \times 10^3$ [s^{-1}]	0.62	1.22	2.37	0.68	1.39	2.73
Y_{peak1}	0.52	0.51	0.48	0.79	0.61	0.59
T_{peak2} [K]	700	716	738	706	726	744
$-(dY/dt)_{\text{peak2}} \times 10^3$ [s^{-1}]	0.17	0.31	0.61	0.25	0.48	0.94
Y_{peak2}	0.05	0.06	0.04	0.15	0.05	0.05
$T_{\text{offset(c)}}$ [K]	588	599	611	587	598	611
Y_c	0.34	0.34	0.33	0.54	0.44	0.42

(sample (b)) at the three heating rates. It is found that the kinetic parameters are the same except for the stoichiometric coefficients (Table 4), which take into account the variation in the chemical composition of the sample, following the torrefaction treatment. In particular, it can be observed that the volatile amount evolved from the decomposition of the pseudo-component hemicellulose diminishes (from 0.37 to 0.18), while the corresponding values for the pseudo-components cellulose and lignin increase (from 0.33 to 0.42 and from 0.17 to 0.20, respectively). Again a small increase in the volatile amounts evolved from the decomposition of the three pseudo-components is observed as the heating rate is increased (average values are reported in Table 4). A good agreement between predicted and measured integral and differential curves is obtained as indicated by the small deviations reported in Table 4 and also shown by the example reported in Fig. 4A and B, including the dynamics of the three pseudo-components, for a heating rate of 5 K/min. A comparison between the predicted and measured differential curves for the various heating rates is shown in Fig. 5.

A further evaluation is carried out for the curves of all the torrefied samples (a)–(e) obtained at 5 K/min in an inert environment, by allowing variations only for the stoichiometric coefficients, obtaining good predictions as indicated by the small deviations reported in Table 4. Only the sample (e), which has undergone severe torrefaction and has a high conversion degree during torrefaction, requires a small variation on the pre-exponential factor for the decomposition of pseudo-cellulose. It is evident that the contribution of pseudo-hemicellulose is progressively reduced (volatile fraction from 0.37 to 0 for sample (e)), while the volatiles evolved from the pseudo-cellulose show a trend similar to the maximum in the peak rate, that is, they first increase (from 0.33 to 0.48 for sample (c)) and then decrease. On the other hand, the volatiles related to the pseudo-lignin always increase (from 0.17 to 0.40). It can be speculated that the changes in the torrefaction conditions, from sample (a) to sample (c), essentially cause a diminution in the contents of hemicellulose in favor of cellulose and lignin (in addition to the charred residue produced by the torrefaction reactions). As the process temperature (and residence time) is further increased (samples (d) and (e)) decomposition of cellulose also begins so that the percentages of the charred residue and lignin in the sample also become higher. The thermal conditions typically established during torrefaction affect the less thermally stable chemical components, hemicellulose and lignin, that starts to degrade already at temperatures around 473 K, although the extent of the reactions is generally higher for the former [13]. It is also reported [35] that the cellulose crystallinity increases for heat treatments above 473 K and degradation reactions begin for

Table 4
Estimated kinetic parameters (activation energy, *E*, pre-exponential factor, *A*, stoichiometric coefficient, *n*) for the degradation in nitrogen of untreated wood and wood torrefied at several process temperatures, T_p, and residence times, t_r (1,2,3: decomposition of pseudo-components hemicellulose, cellulose and lignin) and corresponding deviations between measured and simulated integral (dev$_{\text{TG}}$) and differential (dev$_{\text{DTG}}$) curves.

Parameters	Torrefaction conditions (T_p [K], t_r [min])					
	Untreated wood	(a) 533, 8	(b) 533, 25	(c) 558, 16.5	(d) 583, 8	(e) 583, 25
E_1 [kJ/mol]	100.6					–
A_1 [s^{-1}]	3.60×10^6					–
ν_1	0.37	0.34	0.18	0.06	0.06	–
E_2 [kJ/mol]	213.1					
A_2 [s^{-1}]	4.17×10^{15}					1.26×10^{16}
ν_2	0.33	0.34	0.42	0.48	0.44	0.050
E_3 [kJ/mol]	38.6					
A_3 [s^{-1}]	1.00×10^0					0.75×10^0
ν_3	0.17	0.16	0.20	0.23	0.24	0.40
dev$_{\text{TG}}$ [%]	0.32	0.57	0.73	0.89	0.64	0.69
dev$_{\text{DTG}}$ [%]	1.89	1.76	1.26	2.59	1.70	6.85

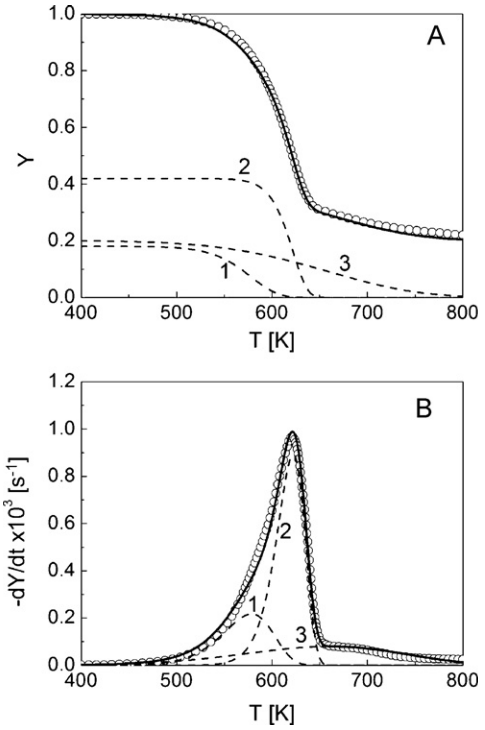

Fig. 4. Comparison between the observed (symbols) and simulated TG (A) and DTG (B) curves (solid lines) for the reference torrefied material (sample (b), Table 1). Thin lines with various styles denote the predicted evolution of the mass fraction and the time derivatives of the pseudo-components (nitrogen, heating rate 5 K/min up to 873 K; 1,2,3: decomposition of pseudo-components hemicellulose, cellulose and lignin).

temperatures above 543 K. However, the kinetic analysis shows that torrefaction does not alter the thermal decomposition reactivity of the modified (partially reacted) components but only the amounts of volatiles produced on further heating. It is possible that the examination of higher heating rates in thermogravimetry would result in significantly different activation energies, especially for the hemicellulose and lignin pseudo-components, for both torrefied and untreated wood [36].

3.3. *Kinetic analysis of the curves obtained in oxidative environment*

The procedure applied to carry out the kinetic evaluation of the curves obtained in air is the same as described above for the measurements made in nitrogen. Thus, thermogravimetric curves for the untreated material obtained at heating rates of 2.5, 5 and 10 K/min are analyzed first, using as starting values for the kinetic parameters those determined for washed fir wood [27]. The optimization procedure again leads to parameters (Table 5, average values for the stoichiometric coefficients) that are slightly different as a consequence of the wood species and pre-treatment difference in the first place. However, for the devolatilization stage, variations are small (activation energies of 101, 213 and 121 kJ/mol, for the oxidative decomposition of the pseudo-components hemicellulose, cellulose and lignin versus values of 106, 226 and 104 kJ/mol, respectively). Comparable values are also obtained for the two reactions related to the oxidation stage (106 and 174 kJ/mol for char devolatilization and oxidation versus 114 and 193 kJ/mol, respectively). The agreement between predictions and measurements is good as indicated by the small deviations (Table 5) and the example shown in Fig. 6A and B, which also includes the component dynamics.

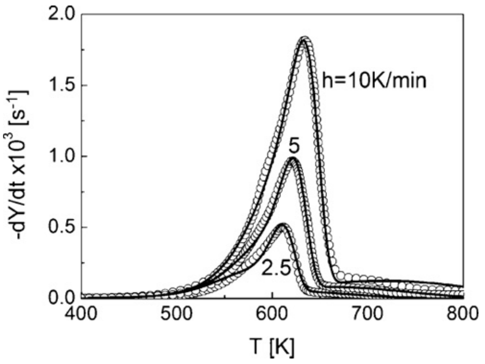

Fig. 5. Comparison between the observed (symbols) and simulated DTG curves (solid lines) for the reference torrefied material (sample (b), Table 1) at various heating rates, *h* (nitrogen, final temperature 873 K).

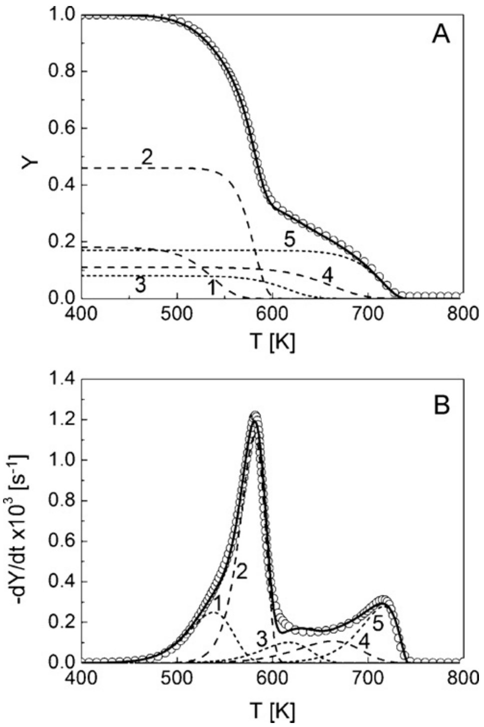

Fig. 6. Comparison between the observed (symbols) and simulated TG (A) and DTG (B) curves (solid lines) for untreated wood. Thin lines with various styles denote the predicted evolution of the mass fraction and the time derivatives of the pseudo-components (air, heating rate 5 K/min up to 873 K; 1,2,3: decomposition of pseudo-components hemicellulose, cellulose and lignin; 4,5 devolatilization and oxidation of char).

A comparison between the two sets of kinetic data obtained for untreated wood devolatilization in nitrogen (Table 4) and air (Table 5) shows that, for the first two reactions, the activation energies are the same. So the anticipation in the devolatilization process observed in air can be adequately described by variations in the pre-exponential factors. Also, the enhanced overlap between reactions gives rise to modified values of the stoichiometric coefficients. More precisely, the volatiles that can be associated with the decomposition of the pseudo-hemicellulose in air are significantly reduced (about 0.18 versus 0.37) to the advantages of the contribution generated from the pseudo-cellulose. On the contrary, the kinetic parameters associated with the devolatilization of the pseudo-lignin are highly different between the two data sets (an activation energy of 106 kJ/mol in air versus a value of 39 kJ/mol in nitrogen). It is possible that, in air, the process of lignin devolatilization is also associated with the beginning of char devolatilization

Table 5
Estimated kinetic parameters (activation energy, E, pre-exponential factor, A, stoichiometric coefficient, n, reaction order n_5) for the degradation in air of untreated wood and wood torrefied at several process temperatures, T_p, and residence times, t_r (1,2,3: decomposition of pseudo-components hemicellulose, cellulose and lignin; 4,5 devolatilization and oxidation of char) and corresponding deviations between measured and simulated integral (dev_{TG}) and differential (dev_{DTG}) curves.

Parameters	Torrefaction conditions (T_p [K], t_r [min])					
	Untreated wood	(a) 533, 8	(b) 533, 25	(c) 558, 16.5	(d) 583, 8	(e) 583, 25
E_1 [kJ/mol]	100.6					–
A_1 [s^{-1}]	2.0×10^7					–
ν_1	0.18	0.12	0.05	0.03	0.02	0.00
E_2 [kJ/mol]	213.1					
A_2 [s^{-1}]	8.80×10^{16}					2.00×10^{17}
ν_2	0.46	0.49	0.53	0.49	0.47	0.10
E_3 [kJ/mol]	121.2					
A_3 [s^{-1}]	5.69×10^7					
ν_3	0.08	0.08	0.08	0.09	0.09	0.16
E_4 [kJ/mol]	106.2					
A_4 [s^{-1}]	5.60×10^5					
ν_4	0.11	0.11	0.11	0.13	0.15	0.23
E_5[kJ/mol]	174.4	197.9				
A_5 [s^{-1}]	9.32×10^9	4.32×10^{11}				
n_5	0.64	0.60				
ν_5	0.17	0.21	0.23	0.26	0.27	0.51
dev_{TG} [%]	0.35	0.70	0.84	0.88	0.75	1.44
dev_{DTG} [%]	1.60	2.49	2.92	2.92	3.12	3.02

as, in this case, the rates of weight loss are significantly higher (see Fig. 1B and Fig. 2B).

The kinetic evaluation of the curves obtained for the reference torrefied wood in air at the various heating rates is made using as starting values for the kinetic parameters those already determined for untreated wood. It is found that the first stage of oxidative degradation can be well described by allowing variations on the stoichiometric coefficients only (Table 5, average values for the stoichiometric coefficients). In other words, it appears that reactivity in oxidative decomposition is again not altered significantly by the torrefaction process although the relative percentages of volatiles evolved from the three pseudo-components are different. As already observed for thermal decomposition, there is a large decrease in the amounts of volatiles generated from the pseudo-hemicellulose (0.05 versus 0.18 for untreated wood) to advantage of the pseudo-cellulose (0.53 versus 0.46 for untreated wood) with a constant contribution from pseudo-lignin (this can be due to a simultaneous enhancement in the decomposition of this component during torrefaction). The step of char devolatilization can also be well described by the parameters already determined for untreated wood (Table 5). Instead, for the actual oxidation step, the description of the curves of torrefied wood requires modifications in the activation energy (a value of 198 kJ/mol versus 174 kJ/mol for untreated wood), pre-exponential factor (4.32×10^{11} versus $9.32 \times 10^9 \text{s}^{-1}$) and reaction order (0.6 versus 0.64). The agreement between predictions and measurements is good as shown by the small deviations reported in Table 5 and the example reported in Fig. 7A and B for a heating rate of 5 K/min, also showing component dynamics. A comparison for the predicted and measured differential curves obtained at various heating rates is shown in Fig. 8.

The thermogravimetric curves of all the torrefied samples obtained at 5 K/min in air can also be well described by the same set of parameters of five reaction mechanism determined for the reference torrefied material by allowing variations on the stoichiometric coefficients only, again with the exception of sample (e) (Table 5). It can be observed that the amounts of volatiles generated from the oxidative decomposition of pseudo-hemicellulose continuously decrease as the torrefaction conditions become more severe, with the contributions associated with the other two pseudo-components attaining a maximum for the samples (b) (cellulose) and (e) (lignin). These results are qualitatively similar to those already found for thermal decomposition. Also, the more severe the torrefaction conditions are the larger the amounts of volatiles generated from char devolatilization and oxidation.

Torrefaction does not alter the oxidative decomposition reactivity of the modified wood components, but the thermal stability of the product char is different as indicated by the peak rates displaced at higher temperatures and the higher activation energy of the oxidation reaction compared with the results obtained for untreated wood. Modifications are, however, small and the kinetic parameters are still in the range of values typically obtained for

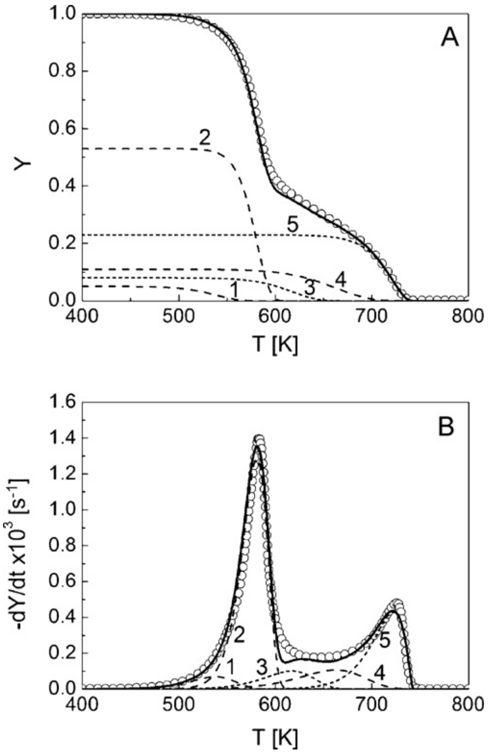

Fig. 7. Comparison between the observed (symbols) and simulated TG (A) and DTG (B) curves (solid lines) for the reference torrefied material (sample (b), Table 1). Thin lines with various styles denote the predicted evolution of the mass fraction and the time derivatives of the pseudo-components (air, heating rate 5 K/min up to 873 K; 1,2,3: decomposition of pseudo-components hemicellulose, cellulose and lignin; 4,5 devolatilization and oxidation of char).

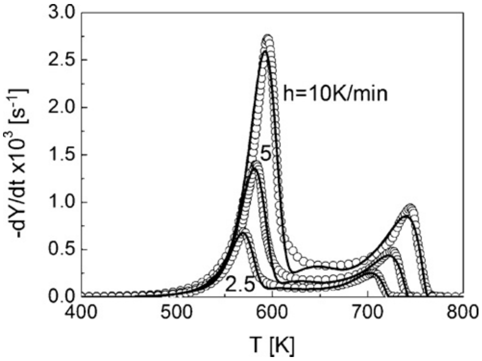

Fig. 8. Comparison between the observed (symbols) and simulated DTG curves (solid lines) for the reference torrefied material (sample (b), Table 1) at various heating rates, *h* (air, final temperature 873 K).

lignocellulosic chars [15]. To point out the differences introduced by torrefaction, a comparison, between the simulated reactivity of char from untreated wood and torrefied wood, in relation to the sole oxidation step, is provided in Fig. 9. Simulations are made with the kinetic parameters already determined (Table 5) and assuming a volatile fraction of 1. It can be seen that differences are negligible at small conversions (below 0.3) and then the char from torrefied wood becomes slightly more reactive.

It is well known [15] that the char reactivity is highly affected by the formation conditions, that is, heating rate, temperature and pressure during pyrolysis, and lignocellulosic precursor nature. A rough evaluation of the apparent heating rates established during the torrefaction process leads to figures that are higher than those of thermal analysis and this may have a beneficial influence of the reactivity of char. Moreover, the different thermal conditions of torrefaction may result in different yields and characteristics of char generated from component decomposition, which also may affect the global char properties and the behavior in combustion. Although extensive investigations about the reactivity of chars generated from hemicellulose, cellulose and lignin are not available, it has been observed that the lignin chars are less reactive than chars from other biomass constituents due to the highly cross-linked and refractory nature [37] and the very small porosity and BET surface area [38]. Therefore, the conditions of torrefaction (heating, rate, temperature, pressure) induce modifications in the structure/chemical composition of the lignocellulosic product that, though not important for devolatilization, may be responsible for some modifications for the reactivity of char in combustion. Finally, the modified content/composition of ashes should also be taken into account.

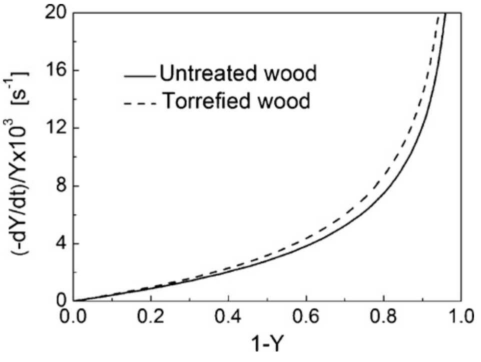

Fig. 9. Predictions of the oxidation reactivity of chars generated from untreated and torrefied wood versus conversion (volatile mass fraction equal to 1 and kinetic parameters of the reaction a5 reported in Table 5).

4. Conclusions

Spruce wood chips have been subjected to torrefaction at a pilot scale by varying the process temperature (533–583 K) and the residence time (8–25 min). As expected, the O and H contents are progressively decreased in favor of the C content with thermal severity of the torrefaction conditions. Torrefied and untreated (for comparison) wood have been studied by means of thermogravimetric analysis in nitrogen and air at different heating rates. It has been found that the thermogravimetric characteristics are largely affected by torrefaction conditions, especially those related to the dynamics of hemicellulose decomposition.

A kinetic evaluation of the measured curves has been carried out to understand the modifications required for the mechanisms currently applied for modeling wood devolatilization and oxidation when applied to describe the conversion dynamics of torrefied materials. The results of the analysis show that the widely applied mechanism, consisting of three parallel reactions for the devolatilization stage, for the pseudo-components hemicellulose, cellulose and lignin, and, in air, of two additional reactions for char devolatilization and oxidation is still applicable.

From the kinetic analysis carried out, it appears that the torrefaction pretreatment does not affect the decomposition behavior of the wood pseudo-components but only their relative amounts. It can be hypothesized that the possible modifications experienced by the wood components during torrefaction, such as partial decomposition, reduction in the polymerization degree and increased crystallinity, do not influence the successive weight loss behavior. Indeed, the activation energies and the pre-exponential factors of the three-step devolatilization mechanism remain unvaried with respect to untreated wood. Instead, the amounts of volatiles evolved from the decomposition of the three pseudo-components, hemicellulose, cellulose and lignin, are highly influenced by the thermal severity established during the torrefaction stage. More precisely, as the temperature and/or the residence time during torrefaction are increased, the contents of hemicellulose are progressively reduced initially to the advantage of both cellulose and lignin and then of lignin only. In general, the yields of char generated from the decomposition stage of torrefied material increase with the thermal severity of the torrefaction process because of the successively larger extent of devolatilization reactions.

The decomposition stage in oxidative environments is also not significantly affected in relation to the reactivity of the three main pseudo-components by the torrefaction pre-treatment but again only in relation to their relative percentages. However, compared with the results obtained for inert atmospheres, the decomposition process occurs at lower temperatures and the overlap between the decomposition of the hemicellulose and cellulose components is enhanced. For the decomposition of the pseudo-components hemicellulose and cellulose, the activation energies remain the same while for the lignin pseudo-component model modifications are required (activation energy of 106 kJ/mol versus 39 kJ/mol), most likely owing to the beginning of char devolatilization.

Weight loss curves of torrefied wood in air, in addition to the first zone of oxidative decomposition, also show a second zone where char devolatilization and oxidation occur. Compared with char generated from untreated wood, the char produced from torrefied wood presents a different thermal stability that appears as an oxidation peak displaced at higher temperatures followed by a more sharp decay. In terms of kinetic parameters these features give rise to higher activation energy (198 versus 174 kJ/mol) and a lower reaction order (0.6 versus 0.64), which are still in the range of values typically reported for lignocellulosic materials. These kinetic parameters are un-variant with the torrefaction conditions, provided modifications in the amounts of volatiles generated from the two reaction steps. Changes in the thermal conditions of char formation and relative yields from the partial decomposition of wood components are possible causes for the difference. These aspects deserve further investigations but it is important to point out that torrefaction, although not important in relation to the rate of volatile release during the devolatilization stage, may influence the activity of the heterogeneous reactions of char which, being the slowest, determine the capacity of combustors and gasifiers.

Acknowledgments

Martin Nordwaeger and Ingemar Olofsson, Energy Technology and Thermal Process Chemistry, Umeå University, are acknowledged for producing the torrefied material and for comments on the manuscript. Financial support from the Swedish Energy Agency (STEM) is gratefully acknowledged. We also thank Bio4Energy, a strategic research environment appointed by the Swedish government, for supporting this work.

References

[1] J. Joelsson, On Swedish bioenergy strategies to reduce CO_2 emissions and oil use, Doctoral Thesis, Mid Sweden University, 2011. ISBN: 978-91-86694-46-3.

[2] R.M. Swanson, J.A. Satrio, R.C. Brown, A. Platon, D.D. Hsu, Techno-economic analysis of biofuels production based on gasification, Technical report, NREL/TP-6A20-46587, National Renewable Energy Laboratory, 2010.

[3] A. van der Drift, H. Boerrigter, M.K. Coda, K. Hemmes, Entrained flow gasification of biomass – ash behaviour, feeding issues, and system analyses, Technical report, ECN-C-04-039, 2004.

[4] H. Boerrigter, Economy of Biomass-to-Liquids (BTL) plants – an engineering assessment, Technical report, ECN-C-06-019, 2006.

[5] B.G. Miller, Coal Energy Systems, Elsevier, Oxford, United Kingdom, 2005, ISBN: 0-12-497451-1.

[6] NETL Gasification Technologies, Worldwide Gasification Database, National Energy Technology Laboratory, US Department of Energy, Washington DC, 2010, http://www.netl.doe.gov/technologies/coalpower/gasification/worlddatabase/index.html.

[7] M.J.C. van der Stelt, H. Gerauser, J.H.A. Kiel, K.J. Ptasinski, Biomass upgrading by torrefaction for the production of biofuels: a review, Biomass Bioenergy 35 (2011) 3748–3762.

[8] B. Arias, C. Pevida, J. Fermoso, M.G. Plaza, F. Rubiera, J.J. Pis, Influence of torrefaction on the grindability and reactivity of woody biomass, Fuel Process. Technol. 89 (2008) 169–175.

[9] T.G. Bridgeman, J.M. Jones, I. Shield, P.T. Williams, Torrefaction of reed canary grass, wheat straw and willow to enhance solid fuel qualities and combustion properties, Fuel 87 (2008) 844–856.

[10] J. Wannapeera, B. Fungtammasan, N. Worasuwannarak, Effects of temperature and holding time during torrefaction on the pyrolysis behaviors of woody biomass, J. Anal. Appl. Pyrolysis 92 (2011) 99–105.

[11] C. Couhert, S. Salvador, J.M. Commandre, Impact of torrefaction on syngas production from wood, Fuel 88 (2009) 2286–2290.

[12] G. Várhegyi, M.J. Antal, E. Jakab, P. Szabo, Kinetic modelling of biomass pyrolysis, J. Anal. Appl. Pyrolysis 42 (1997) 73–87.

[13] C. Di Blasi, Modeling chemical and physical processes of wood and biomass pyrolysis, Prog. Energy Combust. 34 (2008) 47–90.

[14] J.A. Conesa, A. Marcilla, J.A. Caballero, R. Font, Comments on the validity and utility of the different methods for kinetic analysis of thermogravimetric data, J. Anal. Appl. Pyrolysis 58–59 (2001) 617–633.

[15] C. Di Blasi, Combustion and gasification rates of lignocellulosic chars, Prog. Energy Combust. 35 (2009) 121–140.

[16] M.J. Antal, G. Várhegyi, Cellulose pyrolysis kinetics: the current state of knowledge, Ind. Eng. Chem. Res. 34 (1995) 703–717.

[17] M.G. Gronli, A theoretical and experimental study of the thermal degradation of biomass, PhD Thesis, NTNU, Trondheim, Norway, 1996.

[18] J.A. Caballero, J.A. Conesa, R. Font, A. Marcilla, Pyrolysis kinetics of almond shells and olive stones considering their organic fractions, J. Anal. Appl. Pyrolysis 42 (1997) 159–175.

[19] R. Abreu Naranjo, J.A. Conesa, E.E. Foppa Pedretti, O. Romero Romero, Kinetic analysis: simultaneous modeling of pyrolysis and combustion processes of dichrostachys cinerea, Biomass Bioenergy 36 (2012) 170–175.

[20] J.J. Manya, E. Velo, L. Puigjaner, Kinetics of biomass pyrolysis: a reformulated three-parallel reaction model, Ind. Eng. Chem. Res. 42 (2003) 434–441.

[21] M.G. Gronli, G. Várhegyi, C. Di Blasi, Thermogravimetric analysis and devolatilization kinetics of wood, Ind. Eng. Chem. Res. 41 (2002) 4201–4208.

[22] G. Várhegyi, M.G. Gronli, C. Di Blasi, Effects of sample origin, extraction and hot water washing on the devolatilization kinetics of chestnut wood, Ind. Eng. Chem. Res. 43 (2004) 2356–2367.

[23] C.J. Gomez, J.J. Manya, E. Velo, L. Puigjaner, Further application of a revisited summative model for kinetics of biomass pyrolysis, Ind. Eng. Chem. Res. 43 (2004) 901–906.

[24] C.J. Gomez, G. Várhegyi, L. Puigjaner, Slow pyrolysis of wood residues and herbaceous biomass crop: a kinetic study, Ind. Eng. Chem. Res. 44 (2005) 6650–6660.

[25] C. Branca, C. Di Blasi, Devolatilization and combustion kinetics of wood chars, Energy Fuels 17 (2003) 1609–1615.

[26] C. Branca, C. Di Blasi, Global intrinsic kinetics of wood oxidation, Fuel 83 (2004) 81–87.

[27] C. Branca, C. Di Blasi, Oxidative devolatilization kinetics of wood impregnated with two ammonium salts, Fire Safety J. 43 (2008) 317–324.

[28] C. Branca, C. Di Blasi, Combustion kinetics of secondary biomass chars in the kinetic regime, Energy Fuels 24 (2010) 5741–5750.

[29] G. Várhegyi, P. Szabo, M.J. Antal, Kinetics of charcoal devolatilization, Energy Fuels 16 (2002) 724–731.

[30] G. Várhegyi, E. Meszaros, M.J. Antal, J. Bourke, E. Jakab, Combustion kinetics of corncob charcoal and partially demineralized corncob charcoal in the kinetic regime, Ind. Eng. Chem. Res. 45 (2006) 4962–4970.

[31] C. Branca, C. Di Blasi, Parallel- and series-reaction mechanisms of wood and char combustion, Therm. Sci. 8 (2004) 51–63.

[32] G. Várhegyi, Z. Sebestyen, Z. Czegeny, F. Lezsovits, S. Konczol, Combustion kinetics of biomass material in the kinetic regime, Energy Fuels 26 (2012) 1323–1335.

[33] C. Branca, C. Di Blasi, H. Horacek, Analysis of the combustion kinetics and the thermal behavior of an intumescent system, Ind. Eng. Chem. Res. 41 (2002) 2104–2114.

[34] F. Shafizadeh, A.G.W. Bradbury, Thermal degradation of cellulose in air and nitrogen at low temperatures, J. Appl. Polym. Sci. 2 (1979) 1431–1442.

[35] T. Melkior, S. Jacob, G. Gerbaud, S. Hediger, L. Le Pape, L. Bonnefois, M. Bardet, NMR analysis of the transformations of wood constituents by torrefaction, Fuel 92 (2012) 271–280.

[36] C. Branca, A. Albano, C. Di Blasi, Critical evaluation of wood devolatilization mechanisms, Thermochim. Acta 429 (2005) 133–141.

[37] R.K. Sharma, J.B. Wooten, V.L. Baliga, X. Lin, W.G. Chan, M.P. Hajaligol, Characterization of chars from pyrolysis of lignin, Fuel 83 (2004) 1469–1482.

[38] L. Khezami, A. Chetouani, B. Taouk, R. Capart, Production and characterization of activated carbon from wood components in powder: cellulose, lignin, xylan, Powder Technol. 157 (2005) 48–56.